Neutron Dosimetry for Low Dose Rate Cf-252 AT Sources and Adherence to Recent Clinical Dosimetry Protocol for Brachytherapy

$CONF-980403--$

Mark J. Rivard, Jacek G. Wierzbicki, and Frank Van den Heuvel
Department of Radiation Oncology
Wayne State University
3990 John R Road
Detroit, MI 48201

Rodger C. Martin
Chemical Technology Division
Oak Ridge National Laboratory*
P.O. Box 2008
Oak Ridge, TN 37831-6385

RECEIVED

MAR 0 6 1998

OSTI

19980406 137

DISTRIBUTION OF THIS DOCUMENT IS UNLIMITED

MASTER

DISCLAIMER

Neutron Dosimetry for Low Dose Rate Cf-252 AT Sources and Adherence to Recent Clinical Dosimetry Protocol for Brachytherapy

Mark J. Rivard, Jacek G. Wierzbicki, Frank Van den Heuvel, and Rodger C. Martin

Abstract

In 1995, the American Association of Physicists in Medicine Task Group 43 (AAPM TG-43) published a protocol obsoleting all mixed-field radiation dosimetry for Cf-252. Recommendations for a new brachytherapy dosimetry formalism made by this Task Group favor quantification of source strength in terms of air kerma rather than apparent Curies or other radiation units. Additionally, representation of this dosimetry data in terms of radial dose functions, anisotropy functions, geometric factors, and dose rate constants are in an angular and radial (spherical) coordinate system as recommended, rather than the along-away dosimetry data (Cartesian coordinate system) currently available. This paper presents the initial results of calculated neutron dosimetry in a water phantom for a Cf-252 applicator tube (AT) type medical source soon available from Oak Ridge National Laboratory (ORNL).

1. INTRODUCTION

The dosimetry of Cf-252 sources has been reasonably characterized over the years by many authors [1-5]. These data have generally been expressed in the old brachytherapy formalism employing apparent activity, A, and the exposure rate constant, Γ, as in Equation 1. To our knowledge, this paper presents the first instance where TG-43 formalism (spherical coordinate system, etc.) was used to express Cf-252 dosimetry data in terms of the kinetic energy released in air (air kerma). One may not directly compare these Cf-252 neutron data with Cf-252 photon data or from other sources as the mechanisms of interaction are quite different for each type of radiation.

$$D(r) = (\mu_{EN} / \rho) \, \Gamma \, A / r^2 \tag{1}$$

2. BACKGROUND

2.1 TG-43 PROTOCOL AND Cf-252 NEUTRON DOSIMETRY

The current brachytherapy formalism, as applied to neutron dosimetry and recommended by TG-43 [6], follows in Equation 2 where the dose rate, $D_N(r,\theta)$, is equal to the product of: air kerma strength, S_{KN}, dose rate constant, Λ_N, radial dose function, $g_N(r)$, anisotropy function, $F_N(r,\theta)$, and ratio of the geometric factor, $G(r,\theta)$, as normalized to 1 cm on the transverse axis (90°), $G(r_0,\theta_0)$.

$$D_N(r,\theta) = S_{KN} \, \Lambda_N \, g_N(r) \, F_N(r,\theta) \, [\, G(r,\theta) / G(r_0,\theta_0) \,] \tag{2}$$

The air kerma strength, S_{KN}, is a measure of how much radioactive material is on hand, and is the product of the air kerma rate, $K_N(r)$, and the measured distance from the source (typically 1 meter), see Equation 3. Air kerma strength units (U) are generally determined by the commercial manufacturer and within 3% of the desired value [7]. However, Cf-252 sources are created at ORNL where source strengths are expressed in terms of mass (μg) of Cf-252 present, as was similarly performed in the past for Ra-226 (i.e. mg-Ra-eq) in which the Curie was originally defined (i.e. 1 Ci / g).

$$S_{KN} = K_N(d) \, d^2 \tag{3}$$

The neutron dose rate constant, Λ_N, is determined by dividing the Cf-252 AT neutron dose rate at 1 cm in water on the transverse axis by the neutron air kerma strength as shown below in Equation 4.

$$\Lambda_N = D_N(r_0,\theta_0) / S_{KN} \tag{4}$$

For photon dosimetry, the radial dose function, g(r), accounts for absorption and scatter within the dosimetry medium along the transverse source axis. Though the mechanisms of interactions are different between photons and neutrons, there is still merit in characterizing the dose falloff on the transverse axis ($\theta_0 = 90°$) for Cf-252 sources. Here, $g_N(r)$ is defined as the ratio of neutron dose rate per effect of the geometric factor, normalized to the 1 cm value ($r_0 = 1$), and presented below in Equation 5.

$$g_N(r) = D(r,\theta_0) \, G(r_0,\theta_0) / [\, D(r_0,\theta_0) \, G(r,\theta) \,] \tag{5}$$

For practical calculative and comparative purposes, g(r) is usually expressed as a polynomial as below in Equation 6. Note that the first order term of this equation was incorrectly published in equation 14 of TG-43 by Nath *et al.* [6].

$$g_N(r) = a_0 + a_1 r + a_2 r^2 + a_3 r^3 + a_4 r^4 + a_5 r^5 \tag{6}$$

The geometric factor, $G(r,\theta)$, is used to extract the effects of geometry (proximity, Sievert integral of solid angle, etc.) from the calculated data. Removal of a $1/r^2$ factor would take place if the radioactive entity was approximated as a point source. Currently, there are no instances where clinical dosimetry using a Cf-252 AT type source may be properly approximated as a point source; therefore, an extended source model was needed and a line source is generally adequate. Expression of $G(r,\theta)$ is presented below in Equation 7. Here, β is defined as the angle subtended by the active source ends and the point of interest; the active source length (L), radial distance (r) from active source center, and the angle (θ) between the source long-axis and point of interest are all utilized.

$$G(r,\theta) = \beta / (L \, r \sin \theta) \tag{7}$$

$G(r,\theta)$ for $\theta = 0$ degrees was determined using L'Hôpital's rule [8], this case reduced to:

$$G(r, \theta = 0°) = 1 / [r^2 - (L/2)^2] \tag{8}$$

For the case where $\theta_0 = 90$ degrees, $G(r,\theta_0)$ simplified to:

$$G(r,\theta_0) = 2 \arctan (L/2\,r) / [\, L \, r \,] \tag{9}$$

The remaining geometric cases followed the general form of $G(r,\theta)$:

$$G(r,\theta) = \{\arctan [\, (L/(2\,r\sin\theta)) + \text{arccot}\,\theta \,] + \arctan [\, (L/(2\,r\sin\theta)) - \text{arccot}\,\theta \,]\} / L \, r \sin \theta \tag{10}$$

The anisotropy function, $F_N(r,\theta)$, is used to correct for attenuation and scatter of radiation in the encapsulation and medium. Its effects are extracted from the calculated dosimetry with the geometric factor excluded. This is presented below in Equation 11.

$$F_N(r,\theta) = D_N(r,\theta) \, G(r_0,\theta_0) / [\, D_N(r_0,\theta_0) \, G(r,\theta) \, g_N(r) \,] \tag{11}$$

The anisotropy function can be reduced to an anisotropy factor, $\phi(r)$, by integrating dose over all angles (4π). The anisotropy factor also may be reduced to an anisotropy constant, ϕ, if its behavior is constant as a function of radii.

3. DESCRIPTION

3.1 CALCULATIONAL METHODOLOGY AND Cf-252 AT SOURCE MODEL

The Cf-252 neutron energy spectrum was modeled with distributed MCNP as a Watt fission energy spectrum as recommended in the user's manual [9]. The neutrons were emitted isotropically from a cylindrical source cell which was modeled as the Pd:Cf$_2$O$_3$ cermet matrix. This cylinder was 1.50 cm long, had a 0.615 mm radius, and a mass density of 12 g/cm^3. The source wire as this source was contained within a primary capsule of Pt/Ir-10% mass which had inner and outer diameters of 1.30 and 1.70 mm respectively, and inner and outer lengths of 15.50 and 17.78 mm

respectively. The outer capsule was of identical composition, had inner and outer diameters of 1.80 and 2.80 mm respectively, and inner and outer lengths of 17.82 and 23.14 mm respectively. Note that the inner and outer capsule ends were welded and rounded, and that the active source was not centered lengthwise within either the inner or outer capsules. Further, the 0.635 mm diameter Bodkin eyelet through the outer capsule was also included in the source model. These data were used to facilitate fabrication and registration of ORNL-made Cf-252 AT sources [10]. The air inside the primary and secondary capsules, as well as that in the eyelet, and that used for derivation of air kerma strength (S_{KN}) was modeled using compositions and mass density (0.0012 g / cm^3) from the CRC handbook, and converted to include natural abundance isotopic compositions for each element [11]. The dosimetry phantom was modeled as light water with 0.015% atomic abundance H-2, and a mass density at 37°C of 0.998 g / cm^3. As the source was cylindrically symmetric, the sampling space was created using conics bounded by spheres of two different radii. The ratio of the difference of the inner and outer radii and their mean value was never greater than 0.1%. The conics sampled between zero and 180 degrees with 180 degrees defined as the direction of source center to Bodkin eyelet end. The number of histories (nps), typically 50 million, were such that the dosimetric errors (σ) in each cell were less than 0.5%. Finally, the MCNP TMP card was employed to properly model low energy neutron transport [12].

4. RESULTS

4.1 AIR KERMA STRENGTH

As recommended in TG-43, the air kerma strength, S_{KN}, was determined for Cf-252 AT sources. This was calculated (nps = 5 million) for neutron dosimetry with three different air phantom models to study possible attenuation or geometric effects. Parameters of each model are listed in Table 1, and demonstrated the independence of S_{KN} on the choice of air phantom model. In considering the recoil proton ranges (0.5 and 35 cm) from the most probable neutron energy (0.7 MeV) and largest energy (+10 MeV) neutrons, it was clear that S_{KN} was sufficiently modeled at 100 cm with adequate buildup material for the secondary charged particles in transient charged particle equilibrium [13].

Table 1. Air kerma phantom parameters for Cf-252 AT neutron dosimetry

Model #	Density (g / cm^3)	Radii Range (cm)	θ Range (degrees)	Mass (g)	S_{KN} (cGy-cm^2 / μg-h)
1	0.0012	± 0.5	± 1.0	2.632	0.332±0.001
2	0.0012	± 3.0	± 1.0	15.791	0.334±0.001
3	0.0012	± 3.0	± 8.0	126.732	0.335±0.001

4.2 DOSE RATE CONSTANT

With $D_N(r_0,\theta_0)$ = 1.873 cGy / h, and S_{KN} = 0.334 U / μg, this gave Λ_N = 5.608 cGy / h-U as outlined above in Equation 4. As the neutron dose rate constant, Λ_N, was both a function of the source geometry and measuring medium, it was expected that this will vary among different Cf-252 sources. However, the neutron air kerma strength, S_{KN}, was not expected to change unless Cf-252 sources are chosen or fabricated in a markedly different manner as here. Here Λ_N was determined for dose in water, but clinical applications may necessitate phantom specific derivations of Λ_N to account for the inequality of kerma between, for instance, water and muscle.

4.3 RADIAL DOSE FUNCTION

The neutron radial dose function, $g_N(r)$, polynomial series expansion parameters are expressed below in Equation 12. This curve is plotted alongside calculated dosimetry data in Figure 1. As the Cf-252 AT type sources were considerably larger than most clinical sources, the radial dose function exhibited supra-linearity behavior for radii less than 0.30 cm due to breakdown of the line source model. An offset of (r − 0.0615) accounting for the active wire radius in the G(r,θ) calculation of $g_N(r)$, yielded a result (not shown) which modeled the supra-linearity behavior to first order.

$$a_0 = 1.0053244 \quad a_1 = 0.0175408 \quad a_2 = -0.0240621 \quad a_3 = 0.0028633 \quad a_4 = -1.506e\text{-}4 \quad a_5 = 3.1e\text{-}6 \qquad (12)$$

Fig. 1. Cf-252 AT neutron dosimetry radial dose function, g(r)

4.4 VARIANCE IN ACTIVE LENGTH AND IMPACT ON THE RADIAL DOSE FUNCTION

As the nature of fabrication for these sources is more complicated than standard photon emitting sources, there may be variation in the active length (L) among the sources [14,15]. Since the radial dose function, $g_N(r)$, is intrinsically related to $G(r,\theta)$ in Equation 5, and is later shown that Cf-252 neutron dosimetry was also dependent on $G(r,\theta)$, one must therefore examine the dosimetric dependence accounting for uncertainties in L. In Table 2, variations in L for 1.5 ± 0.05 cm are presented, and it is shown that fabrication errors of ± 0.05 cm perturbed g(r) about 2% at a distance of ½ cm on the transverse source axis. For distances greater than 1 cm, the perturbation was less than 1%; this perturbation quickly decreased for increasing radii. Robert McMahon of ORNL has measured the actual variances in active lengths during the pre-encapsulation phase of production, and determined that for a recent fabrication run of seventeen Cf-252 AT sources one standard deviation was 0.011 cm [16]. At a prescription distance of ½ cm, there can be expected to be no more than 0.5% variance among the group of Cf-252 AT sources recently produced by ORNL.

Table 2. Impact on $g_N(r)$ for varying Cf-252 source wire active lengths (L)

Radii (cm)	L=1.45	L=1.46	L=1.47	L=1.48	L=1.49	L=1.50	L=1.51	L=1.52	L=1.53	L=1.54	L=1.55
0.15	0.971	0.977	0.983	0.989	0.994	1.000	1.006	1.011	1.017	1.023	1.029
0.25	0.975	0.980	0.985	0.990	0.995	1.000	1.005	1.010	1.015	1.020	1.025
0.50	0.982	0.986	0.989	0.993	0.996	1.000	1.004	1.007	1.011	1.014	1.018
0.75	0.988	0.990	0.993	0.995	0.998	1.000	1.002	1.005	1.007	1.010	1.012
1.00	0.992	0.993	0.995	0.997	0.998	1.000	1.002	1.003	1.005	1.007	1.009
1.50	0.995	0.996	0.997	0.998	0.999	1.000	1.001	1.002	1.003	1.004	1.005
2.00	0.997	0.998	0.998	0.999	0.999	1.000	1.001	1.001	1.002	1.002	1.003
3.00	0.999	0.999	0.999	1.000	1.000	1.000	1.000	1.001	1.001	1.001	1.001
5.00	1.000	1.000	1.000	1.000	1.000	1.000	1.000	1.000	1.000	1.000	1.000
10.0	1.000	1.000	1.000	1.000	1.000	1.000	1.000	1.000	1.000	1.000	1.000

4.5 GEOMETRIC FACTOR

Results of select calculated geometric factors for the general case with θ and for θ_0 are presented below in Tables 3 and 4. Some values were not available (NA) due to their location within the source encapsulation.

Table 3. Select calculated $G(r,\theta)$ for Cf-252 AT neutron dosimetry

Radii (cm)	$\theta = 0^o$	$\theta = 5^o$	$\theta = 10^o$	$\theta = 20^o$	$\theta = 30^o$	$\theta = 45^o$	$\theta = 60^o$
0.25	NA	94.1248	46.2558	22.5366	14.8417	10.0088	7.8999
0.50	NA	50.6477	24.1171	11.1380	7.0769	4.6449	3.6314
1.00	2.2857	2.2211	2.0617	1.6855	1.3903	1.1121	0.9591
2.00	0.2909	0.2904	0.2887	0.2827	0.2743	0.2606	0.2491
5.00	0.0409	0.0409	0.0409	0.0408	0.0406	0.0403	0.0400
10.0	0.0101	0.0101	0.0101	0.0100	0.0100	0.0100	0.0100

Table 4. Calculated $G(r,\theta_0)$ for Cf-252 AT neutron dosimetry

Radii (cm)	$G(r,\theta_0)$	Radii (cm)	$G(r,\theta_0)$	Radii (cm)	$G(r,\theta_0)$	Radii (cm)	$G(r,\theta_0)$
0.15	12.208	1.10	0.725	2.90	0.116	5.75	0.030
0.20	8.735	1.20	0.621	3.00	0.109	6.00	0.028
0.25	6.662	1.30	0.537	3.10	0.102	6.25	0.025
0.30	5.290	1.40	0.468	3.20	0.096	6.50	0.024
0.35	4.321	1.50	0.412	3.30	0.090	6.75	0.022
0.40	3.603	1.60	0.365	3.40	0.085	7.00	0.020
0.45	3.053	1.70	0.326	3.50	0.080	7.25	0.019
0.50	2.621	1.80	0.292	3.60	0.076	7.50	0.018
0.55	2.274	1.90	0.264	3.70	0.072	7.75	0.017
0.60	1.991	2.00	0.239	3.80	0.068	8.00	0.016
0.65	1.757	2.10	0.218	3.90	0.065	8.25	0.015
0.70	1.562	2.20	0.199	4.00	0.062	8.50	0.014
0.75	1.396	2.30	0.183	4.25	0.055	8.75	0.013
0.80	1.255	2.40	0.168	4.50	0.049	9.00	0.012
0.85	1.134	2.50	0.155	4.75	0.044	9.25	0.012
0.90	1.029	2.60	0.144	5.00	0.040	9.50	0.011
0.95	0.938	2.70	0.134	5.25	0.036	9.75	0.010
1.00	0.858	2.80	0.125	5.50	0.033	10.00	0.010

4.6 ANISOTROPY FUNCTION

Using the calculated neutron dosimetry data and calculated geometric factor, the anisotropy function, $F_N(r,\theta)$, was determined from Equation 13. A few select values of $F_N(r,\theta)$ are given below in Table 5. In comparing $F_N(r,\theta)$ with $F(r,\theta)$ for photon emitting radionuclides listed in TG-43, it is clear that Cf-252 neutrons are much less reactive with the encapsulating materials as evidenced by comparisons of the axial ($\theta = 0°$ to $10°$) anisotropy function data [6].

$$F_N(r,\theta) = D_N(r,\theta)\ G(r,\theta_0) / [D_N(r,\theta_0)\ G(r,\theta)] \qquad (13)$$

Table 5. Select calculated $F_N(r,\theta)$ for Cf-252 AT neutron dosimetry

Radii (cm)	$\theta = 5°$	$\theta = 10°$	$\theta = 20°$	$\theta = 30°$	$\theta = 45°$	$\theta = 60°$	$\theta = 90°$
0.25	NA	NA	NA	NA	1.008	1.004	1.000
0.50	NA	NA	1.023	1.012	1.008	1.006	1.000
0.75	NA	1.012	1.001	1.001	1.000	1.000	1.000
1.00	NA	0.985	0.993	0.997	1.001	1.000	1.000
1.50	0.968	0.978	0.999	0.995	1.002	1.000	1.000
2.00	0.964	0.975	0.995	0.999	1.001	0.999	1.000
3.00	0.961	0.976	0.998	0.998	1.000	1.000	1.000
5.00	0.983	0.974	0.999	0.998	1.000	1.001	1.000
10.0	0.983	0.977	0.995	0.998	1.001	1.000	1.000

4.7 ANISOTROPY FACTOR

The neutron anisotropy factor, $\phi_N(r)$, was calculated in two manners. First, the data from the angular conics used in derivation of $D_N(r,\theta)$ was weighted according to the mass of each volume element to derive equal 4π sampling. Second, an additional run was made which sampled dose between spheres enclosing the source and binned for a given radius. Results of these two approaches were identical given the statistical uncertainty ($\sigma = 0.001$). The anisotropy factor for Cf-252 AT neutron dosimetry is presented below in Figure 2 and Table 6. Due to moderation effects and the relatively large size of the AT sources as compared with other sources commonly used in brachytherapy, the neutron anisotropy factor could not be accurately reduced to an anisotropy constant.
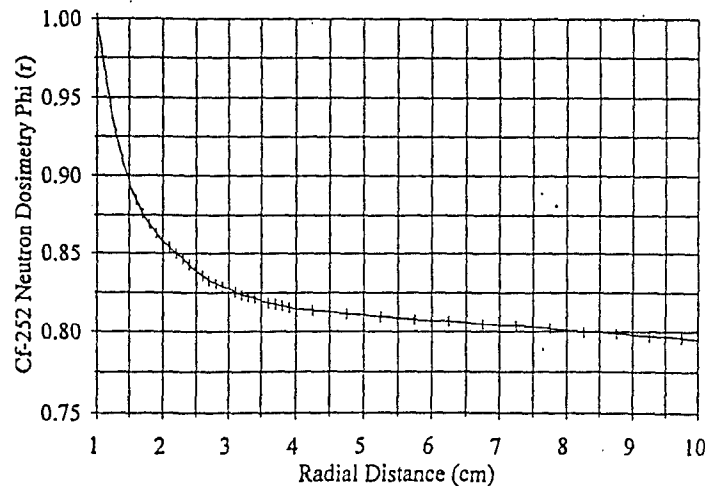

Fig. 2. Cf-252 AT neutron dosimetry anisotropy function, $\phi(r)$

Table 6. Anisotropy factor, $\phi_N(r)$, for Cf-252 AT neutron dosimetry

Radii (cm)	$\phi_N(r)$	Radii (cm)	$\phi_N(r)$	Radii (cm)	$\phi_N(r)$	Radii (cm)	$\phi_N(r)$
1.00	1.000	2.40	0.843	3.80	0.817	7.00	0.804
1.10	0.972	2.50	0.839	3.90	0.816	7.25	0.804
1.20	0.947	2.60	0.836	4.00	0.815	7.50	0.803
1.30	0.927	2.70	0.833	4.25	0.814	7.75	0.802
1.40	0.910	2.80	0.831	4.50	0.813	8.00	0.801
1.50	0.896	2.90	0.829	4.75	0.812	8.25	0.800
1.60	0.885	3.00	0.828	5.00	0.811	8.50	0.800
1.70	0.876	3.10	0.826	5.25	0.810	8.75	0.799
1.80	0.869	3.20	0.824	5.50	0.809	9.00	0.798
1.90	0.863	3.30	0.823	5.75	0.808	9.25	0.797
2.00	0.858	3.40	0.822	6.00	0.807	9.50	0.797
2.10	0.854	3.50	0.820	6.25	0.807	9.75	0.796
2.20	0.850	3.60	0.819	6.50	0.806	10.00	0.795
2.30	0.847	3.70	0.818	6.75	0.805		

5. CONCLUSIONS

For the first time, AT type Cf-252 neutron dosimetry has been expressed in terms of TG-43 formalism. This approach, as compared to the older formalism relying on apparent activity, mass energy absorption coefficient, and exposure rate constant, has demonstrated the independence of angular data (anisotropy function) when removing the solid angle (geometric factor) component of the dosimetry. As the Cf-252 AT type sources were considerably larger than most clinical sources, the radial dose function exhibited supra-linearity behavior for radii less than 0.30 cm due to breakdown of the line source model. Should high dose rate (HDR) type sources be manufactured, the neutron air kerma strength is not expected to vary significantly as compared with that obtained here for AT type Cf-252 source. This AT neutron dosimetry data may now be entered into a modern brachytherapy treatment planning workstation for local use, as well as abroad.

The reference medium of natural water was chosen as a means to adhere to TG-43 protocol, and permit direct comparison with experimental measurements; however, it is known that the effective kerma value for tissue differs markedly from that of water, and care must be taken in the eventual application of these sources for brachytherapy. Further studies will comprehensively determine dosimetry data, in adherence to TG-43 formalism, for many clinically relevant media.

REFERENCES

1. R. D. Colvett, H. H. Rossi, V. Krishnaswamy Dose distribution around a Cf-252 needle, Phys. Med. Biol. 17, 356, 1972

2. V. Krishnaswamy Calculated depth dose tables for Cf-252 sources in tissue, Phys. Med. Biol. 17, 1972.

3. L. L. Anderson Cf-252 physics and dosimetry, Nuc. Sci. Appl. 4, 273, 1986.

4. J. C. Yanch, R. G. Zamenhof Dosimetry of Cf-252 sources for neutron radiotherapy with and without augmentation by boron neutron capture therapy, Radiation Research 131, pp. 243-256, 1992.

5. J. G. Wierzbicki, M. J. Rivard, W. A. Roberts Physics and dosimetry of clinical Cf-252 sources, In: Cf-252: Isotope for 21st Century Radiotherapy, Ed. J. G. Wierzbicki, Kluwer Academic Pub., pp. 25-53, 1997.

6. Nath, R., et al. Dosimetry of interstitial brachytherapy sources: Recommendations of the AAPM Radiation Therapy Committee Task Group No. 43, Med. Phys. 22, pp. 209-234, 1995.

7. Nath, R., et al. Code of practice for brachytherapy physics: Report of the AAPM Radiation Therapy Committee Task Group No. 56, Med. Phys. 24, pp. 1557-1598, 1997.

8. D. J. Struik, Mathematics Teacher 56, pp. 257-260, 1963.

9. J. Briesmeister MCNP4B User's Manual, LANL, H-3, March 20, 1997.

10. ORNL Drawing #N3D017049A245, 1997.

11. The Elements, In: CRC Handbook of Chemistry and Physics, Section F, CRC Press Inc., 1990.

12. M. J. Rivard, J. G. Wierzbicki, F. Van den Heuvel Calculations of the Cf-252 neutron spectrum for various positions and loadings of B-10 and Gd-157 using MCNP4B, American Nuclear Society RPS Division Topical Conf., Nashville, TN, (these proceedings), 1998.

13. ICRU Report 49. Stopping power and ranges for protons and alpha particles, Bethesda, MD, 1993.

14. J. B. Knauer, Jr., R. C. Martin Californium-252 production and neutron source fabrication, In: Cf-252: Isotope for 21st Century Radiotherapy, Ed. J. G. Wierzbicki, Kluwer Academic Pub., pp. 7-24, 1997.

15. Joseph B. Knauer, Jr. Private communication, ORNL, Oak Ridge, TN, 1996.

16. Robert R. McMahon Private communication, ORNL, Oak Ridge, TN, 1997.

Report Number (14) _ORNL/CP--96451_
CONF-980403--
_____
_____

Publ. Date (11) _1997 12_
Sponsor Code (18) _DOE/⬤DP,XF_
UC Category (19) _UC-700, DOE/ER_

DOE